Some Measurements of Attenuation by Rainfall at 18.5 GHz*

By R. A. SEMPLAK and R. H. TURRIN

(Manuscript received November 7, 1968)

We discuss 18.5 GHz attenuation measurements on a 6.4 km path within the Holmdel rain gauge network. The period of measurement includes the summer of 1967 during which many very heavy showers occurred. We examine the data for individual storms separately. There is a marked variability. For example, one shower shows strong evidence of an updraft. The composite results show that $\gamma = 0.041 \sum_i d_i R_i^{1.04}$ where γ is the attenuation per unit length, R_i is the rainfall rate in millimeters per hour measured at the ith rain gauge on the path, and d_i is the distance in kilometers over which the rain rate R_i applies. When examined in detail, this relationship is satisfactory for attenuations < 3 dB per kilometer; however, the higher attenuations exceed this prediction and agree with the relationship $\gamma = 0.055 \langle R \rangle_{av}^{1.09}$ where $\langle R \rangle_{av}$ is the path-average rain rate. Percent-of-time distributions are given for $\langle R \rangle_{av}$, the attenuation, and the duration of attenuation. For this sample of data, the path attenuation exceeds thirty dB 0.03 percent of the time; thus 6.4 kilometers is probably too long for a conventional 18 GHz radio-relay path in New Jersey. All fades observed to date have been associated with rainfall; thus no "selective fading" has as yet been observed on this 6.4 kilometer path.

I. INTRODUCTION

One of the problems encountered in the utilization of the millimeter-wave bands for radio-relay systems is attenuation resulting from precipitation. There is a continued effort to overcome the fundamental inadequacy concerning the knowledge of the propagation environment. Recently a paper by Medhurst, which collects most of the published measurements on microwave attenuation by rain, has shown that there is wide disagreement between observed and calculated values.[1]

This paper discusses measurements at 18.5 GHz on a 6.4 kilometer path that passes above four capacitor-type rain gauges.[2] The gauges are part of a network centered at Bell Laboratories, Crawford Hill, Holmdel, New Jersey.

II. EXPERIMENTAL ARRANGEMENT

Figure 1, which is a portion of the rain-gauge-network map, indicates the location of the 6.4 kilometer propagation path with a dashed line.[3] The dot within each grid indicates the physical location of a rain gauge mounted at the top of a telephone pole, approximately 7.6m above the ground. In particular, the four rain gauges located in grids 9, 17, 25, and 33 are closely associated with the propagation path. The rainfall rates obtained from these gauges are used in the following discussions.

III. EQUIPMENT

The transmitting and receiving antennas are identical 76-cm diameter parabolic reflectors with a 36.8-cm focal length. To minimize waveguide losses, a spash plate fed by circular waveguide is used. The waveguide extends through the vertex of the reflector where a sidewall coupler provides the transition to rectangular k-band guide with vertical polarization in the dominant mode. The antenna gain measured from the rectangular waveguide port, is 39.9 dB. A klystron operating cw with a power output of about 50 mW is used as the source. The transmitter and antenna are in a small equipment house (a slanted fiberglas weather cover window provides the exit for the transmitted beam) at Cliffwood, New Jersey on the Garden State Parkway Authority right-of-way, (grid 9 of Fig. 1). The line-of-sight path has good foreground clearance at both ends. The path loss $(4\pi R/\lambda)^{-2}$ is 134 dB.

The receiver and its antenna are situated in a housing at the northern end of Crawford Hill (grid 33 of Fig. 1). Entry of the transmitted beam is provided by a sloping Mylar window. The receiver consists of a standard balanced converter followed by a low noise FET preamplifier. The single side band noise figure of the converter-preamplifier is 13 dB and the intermediate frequency is 70 MHz. To overcome effects of frequency drifts associated with the klystrons, the receiver is operated in a swept mode. However, this method of operation penalizes the dynamic measuring range by about 5 dB.
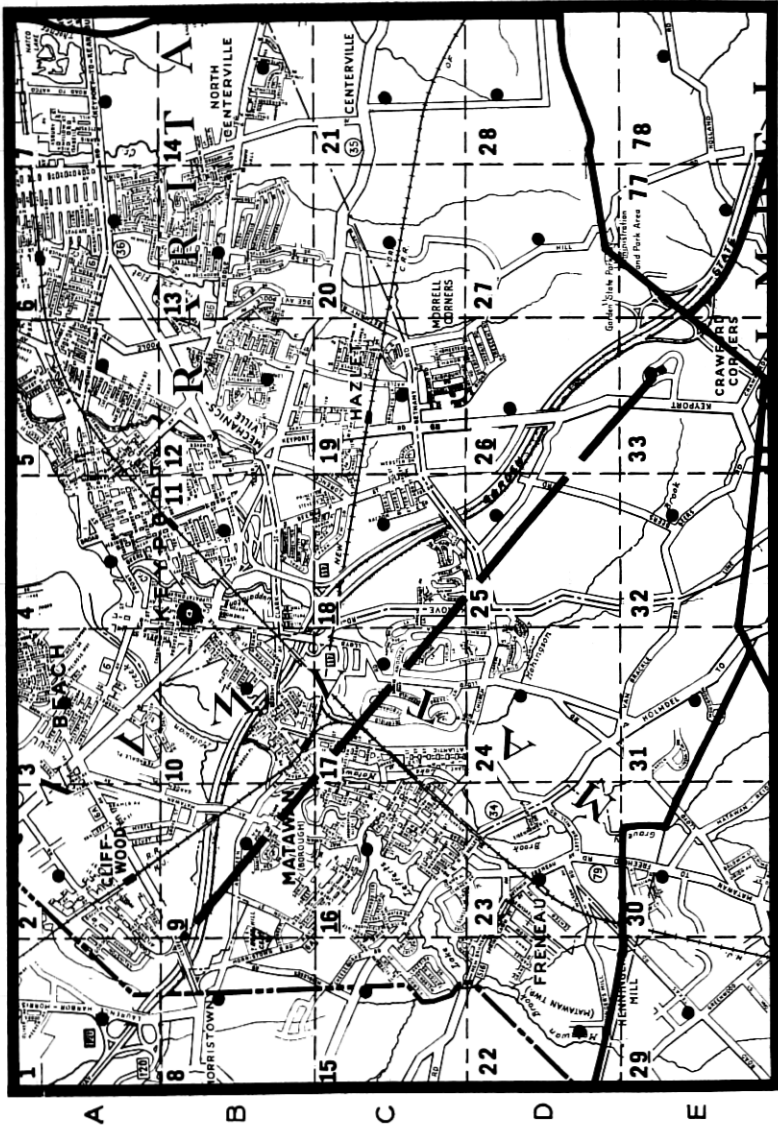
Fig. 1 — An area map showing the physical location of the rain gauges as closed dots. The dashed line is the 18.5 GHz propagation path.

The main IF amplifier is somewhat unique in that it provides an output linear in decibels, over a 50 dB dynamic range. The circuit is British in origin and uses successive transistorized twin gain stages to achieve the log-linear response.[4] The bandwidth of the IF amplifier is about 1.5 MHz and the beating oscillator is swept approximately ± 3 MHz. Visual indication of receiver tuning and sweep is obtained with an oscilloscope monitor of the video detector output. Peak detection of the video pulses provides a dc output (time constant $\approx$ 0.1 sec) which drives an Esterline Angus pen recorder through an FET isolating stage.

Since both rainfall and the resulting attenuation often change rapidly it is almost essential, for purposes of data reduction, to include the propagation data on the same magnetic tape that contains the information from the rain gauges;[3] thus the output of the receiver must be in a form suitable for transmission over a standard unloaded telephone pair, from the receiving site on Crawford Hill to the data collection room in the Crawford Hill laboratory. For this purpose, a voltage-to-frequency converter is used to convert the receiver dc signal into a frequency with a range of 1 KHz to 10 KHz which is suitable for telephone line transmission. The receiver signal is then sampled and recorded on the magnetic tape at the rate of one sample per second.[3]

A permanently installed 18.5 GHz precision variable attenuator is used to calibrate the receiving system. System and path-loss considerations indicate a maximum received signal at the receiving antenna port of the order −38 dBm. The receiver sensitivity is −94 dBm including a 5 dB penalty for sweeping the beating oscillator. Thus the available dynamic range is 56 dB. However, the log-linear amplifier and precision attenuator have a useful dynamic range of 50 dB.

IV. RESULTS

The data discussed here were obtained for the recording period June 23 through October 31, 1967, during which there were twenty-three storms associated with the propagation path.* Complete propagation and rainfall data are available for twenty-one of these storms.

Three storms have been selected to show the marked variability between measured and predicted attenuation on an individual-storm

---

* The summer of 1967 in New Jersey was prolific in heavy showers. During this period, of 3144 hours, a total of 21 inches of rain was measured at Crawford Hill. The annual average rainfall for New Jersey is 40 inches.

basis. Figures 2a, 3a, and 4a show strip chart records obtained during rains on July 21, July 28, and October 25, respectively. An examination of these figures reveals a lack of similarity in both the duration and absolute value of the attenuation.

The measured attenuation is averaged along the path. A comparison is made of the observed attenuations with values predicted from the rainfall rates. For all data to be discussed, the attenuations were read
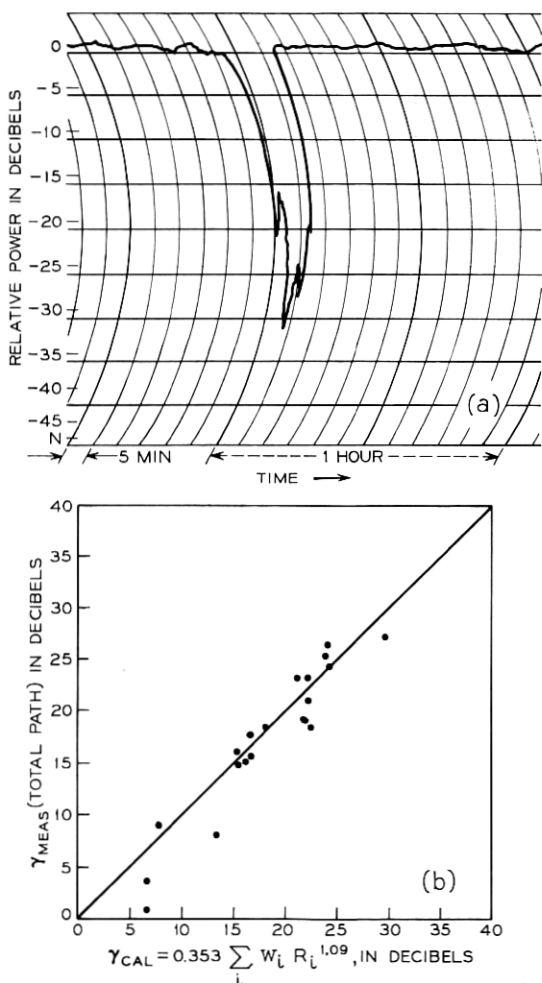

Fig. 2 — (a) Propagation data July 21, 1967. (b) Observed versus predicted path attenuation for July 21, 1967, where the weighing factor $w_i = d_i/6.4$.
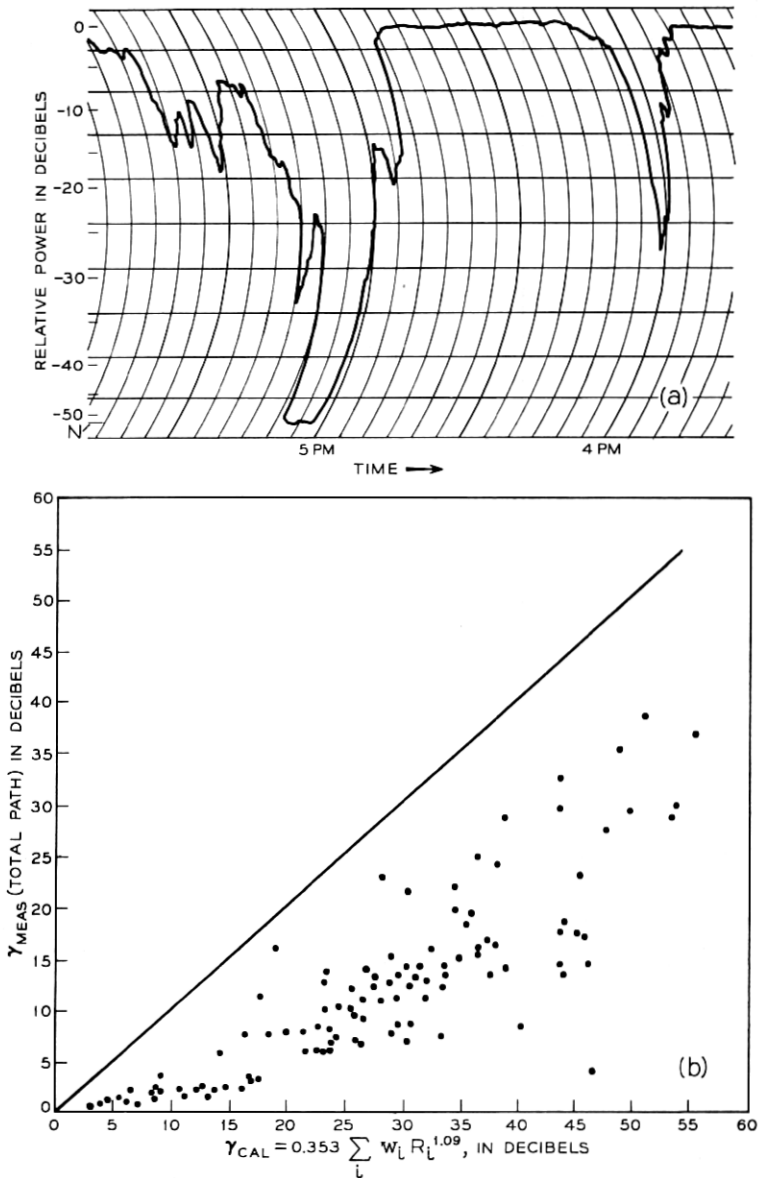
Fig. 3 — (a) Propagation data July 28, 1967. These data are considered as two separate storms and the remarks of the text refer to the second storm beginning about 4:50 P.M. (b) Observed versus predicted path attenuation for July 28, 1967, where the weighing factor $w_i = d_i/6.4$.

once from the magnetic tape during every 30-second interval; the corresponding rainfall rates recorded every ten seconds on the tape were averaged over this same 30-second interval. Plots on individual storms showed that averaging in this manner reduced the scatter in the calculated data. For the predictions, the empirical expression proposed by Gunn and East[5]

$$\gamma = k \sum_i d_i R_i^\alpha \qquad (1)$$

are used. R_i is the rainfall rate measured at the ith rain gauge, d_i the distance in km over which the rain rate R_i applies, $\Sigma_i d_i = d = 6.4$ km, and $i = 1, 2, 3, 4$ is the gauge position.* $k = 0.055$ dB per km and $\alpha = 1.09$ are the values suggested by Gunn and East, based on the Laws and Parsons drop-size distribution.

Heavy rainfalls occur over small areas; it is believed that this area decreases (in general) with increasing rainfall rate. Therefore, unless the gauge spacing is small it is less likely that a heavy rainfall will occur at a gauge but more likely that it will occur between gauges. In such a case, equation (1) tends to underestimate the attenuation. When a heavy rainfall does occur at one gauge (assuming that gauges are not sufficiently closely spaced) equation (1) tends to over-estimate; this is because d_i is fixed and because we assume that the heavy rain rate measured at the ith gauge extends uniformly along d_i. From experience with the network, we have learned that the gauge spacing is somewhat too large to permit resolving the distance associated with some of the very heavy rain rates. Since the rain gauges are sampled every ten seconds, there is also some sampling error in the time domain; this is discussed in the appendix. In particular, note that the four gauges associated with the propagation path are not read consecutively. There is an approximate two second interval between successive readings from the four gauges on the path.

Comparison of the measured attenuation with that calculated using equation (1) for the three selected storms is shown in Figs. 2b, 3b, and 4b. In Fig. 2b, the predicted values agree with the measurements. The agreement is not nearly as good for the rainstorm corresponding to Fig. 3b. The spread of the calculated points is fairly well contained but the indications are that both k and α are too large, that is, we predict an attenuation higher than is actually measured. Both of these constants depend on the drop-size distribution.† The comparison for the last

---

* The appropriate values are $d_1 = 1.933$ km, $d_2 = 1.792$ km, $d_3 = 1.741$ km, and $d_4 = 0.934$ km.
† k is also a function of the fall-velocity of the drops.
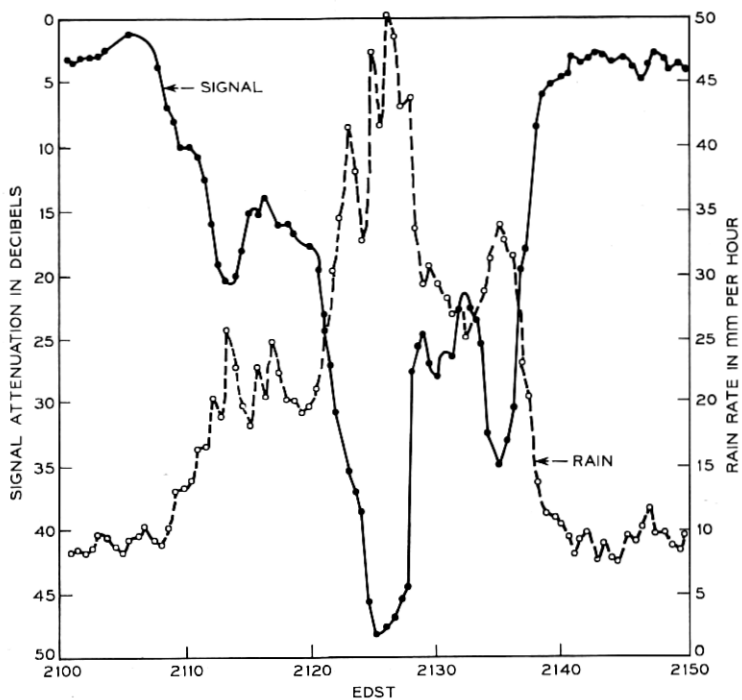
DATA OF OCTOBER 25, 1967
METEOROLOGICAL DATA–FOR 18.5 GHz
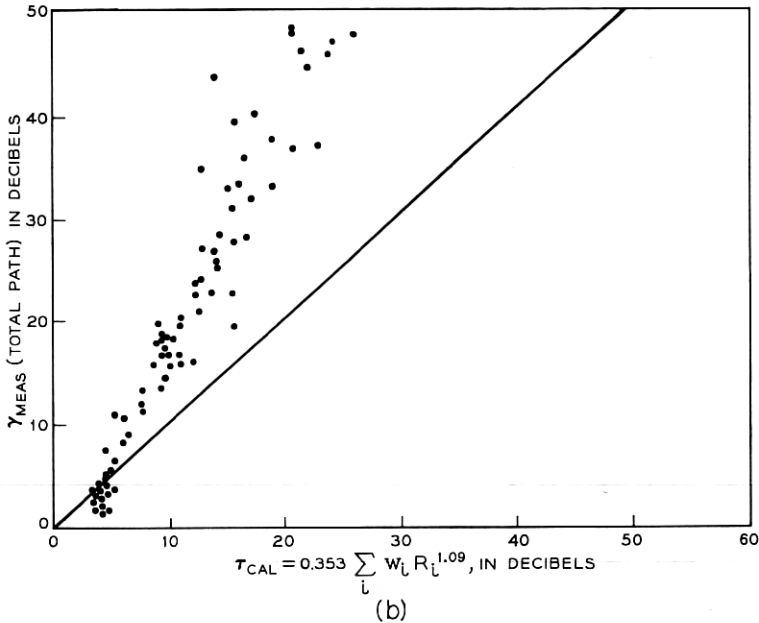6.4 km PATH–CLIFFWOOD–CRAWFORD HILL
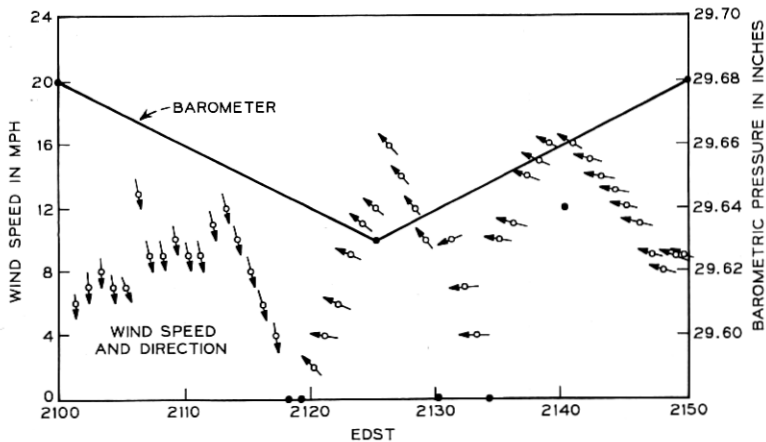
(a)

Fig. 4 — (a) Propagation data for October 25, 1967 along with average rain rate; the lower charts show the pressure and wind at Crawford Hill. (b) Observed versus predicted path attenuation for October 25, 1967, where the weighting factor $w_i = d_i/6.4$.

storm to be considered on an individual basis is shown in Fig. 4b. It is readily apparent that here is a case where the predictions are underestimates; these data are discussed in detail later in this section. For the moment, it is sufficient to say that equation (1) with the above values for k and α tends to overestimate the attenuation in most cases; this is readily seen in Fig. 5 where data for the period of June 23, 1967 to October 25, 1967 have been plotted. Using a nonlinear least squares regression, the values 0.041 ± 0.007 dB per km and 1.042 ± 0.031 are found for k and α respectively.

There are at least three factors which enter into predicting values higher than the measured ones, as in Fig. 5. First, the drop-size distribution often may differ from that commonly used in computation. Secondly, the fall velocity of the drops has a strong effect. The third factor is polarization; since falling rain drops tend to be oblate, attenuation for a vertically polarized electromagnetic wave (as used here) is several percent less than values calculated assuming spherical drops.[5,6]
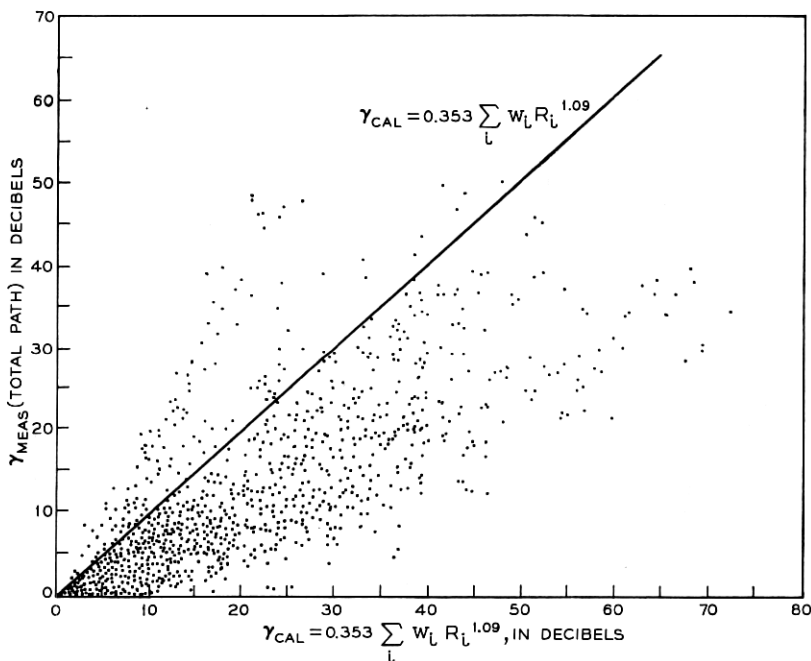
Fig. 5 — Plot of predicted values $\gamma = k \ \Sigma_i \ d_i R_i{}^a$ where $k = 0.055$ dB per kilometer and $\alpha = 1.09$ for all storms during the period June 23 to October 31, 1967.

4.1 *A Special Case*

Let us return to the storm of October 25 (Figs. 4a and b) and examine Fig. 6 which is a plot of measured attenuation versus average rain rate. The dashed lines on this plot are theoretical maximum and minimum attenuations for hypothetical rains containing drops which are all of the same diameter;[1] the diameters specifically chosen are those which produce the maximum and minimum attenuation.* For this case the measured values of attenuation lie well above the theoretical maximum. The spread of the data is small and the solid line is a calculated least squares regression. Since these data differ considerably from the rest of our measurements, an attempt to account for this behavior was made by examining synoptic data for this period.

Large-scale synoptic data indicated the passage of a cold front

---

* Commonly accepted terminal velocities are used in these estimates.

system; this was confirmed by our local wind and pressure measurements shown in Fig. 4a. There is a pressure drop and a wind reversal near the time the attenuation occurred. The classical picture for vertical wind movement at the interface of the cold front is updrafts associated with the retreating warm system and downdrafts in the advancing cold front.[7] Since an updraft decreases the terminal velocity of the rain drops, one has a condition where the density of rain drops in the radio path is greater than is indicated by the rain gauges.

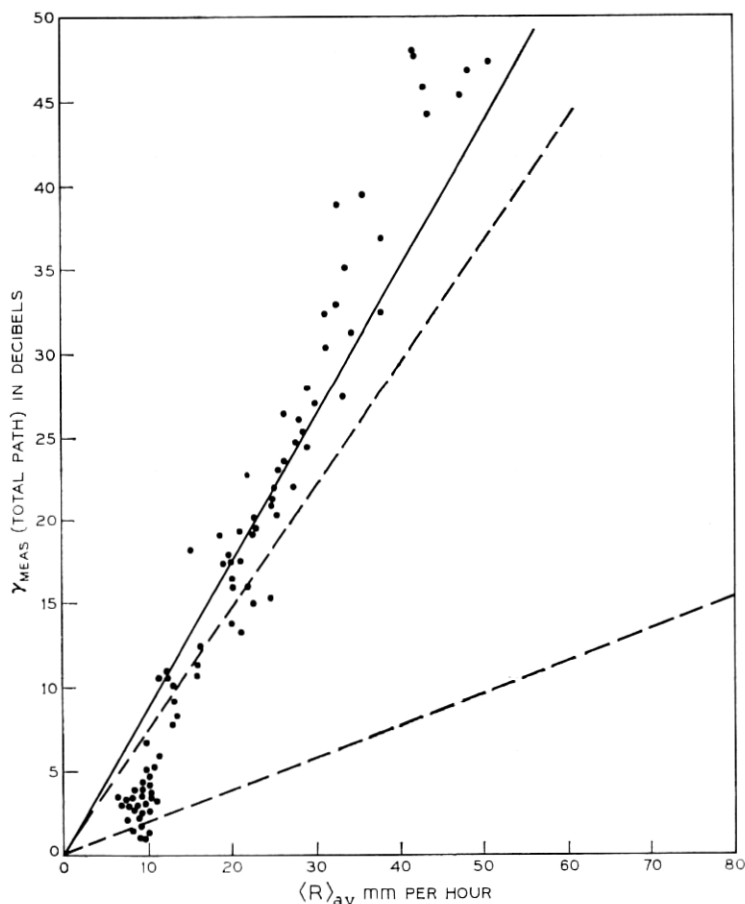Assume for the moment a modest updraft of two miles per hour, that

Fig. 6 — Plot of measured attenuation obtained for October 25, 1967 versus average rain rate.

is, 0.95 m per second. Using this value to correct the rain drops terminal velocities (about 7 m per second) to account for the effect of the updraft, the three points indicated by crosses on Fig. 6 are calculated. If an updraft of 1.9 m per second is assumed, the points indicated by the open circles on Fig. 6 are obtained. A line drawn through the crosses lies close to the calculated regression line and indicates that the updraft is of the order 1 m per second; thus with this assumption, the data are readily explained. Presumably the converse can take place; that is, with a downdraft of 1 m per second the measured attenuation would be about 15 per cent lower than one would estimate.

4.2 *Comparison with Path-Averaged Rain Rate*

Figure 7 shows the totality of the attenuation data plotted as a function of average rain rate $\langle R \rangle_{av}$ (and not the summation of attenuations discussed earlier in Section IV). Since the data obtained from the storm of October 25, (shown by crosses) are reasonably accounted for by an updraft, they are not included in the following discussion. The dashed lines in Fig. 7 are, as in Fig. 6, theoretical maximum and minimum boundaries and the line labeled $\gamma = 0.048 \langle R \rangle_{av}$ dB per km is a linear least square regression for these data;[1] this gives an attenuation directly proportional to average rain rate. To remove any possible influence of improper readings from the rain gauges at low rates, that is, small drops lodging in the trough-type capacitor, these measurements at average rain rates of 10 mm per hour and less have been removed; this accounts for the absence of data points in this range in Fig. 7.

The bulk of the data is well contained within the theoretical boundaries; however, there is a cluster of points near the origin that lies below the boundary. At higher rain rates neither the linear regression line nor the nonlinear regression line labeled $\gamma = 0.04 \langle R \rangle_{av}^{1.04}$ dB per kilometers provide suitable prediction. The line labeled $\gamma = 0.055 \langle R \rangle_{av}^{1.09}$ dB per kilometers, from Gunn and East appears to represent the higher attenuations fairly well; these higher values of attenuation and the associated rainrates are discussed further in Section 4.3.

4.3 *Distributions*

Percent of time distributions for attenuation and average rain rate are plotted in Figs. 8a and b respectively. In addition to the distribution (Fig. 8a) for the summer period, distributions for the period covering spring, fall, and winter and for the full year are shown.
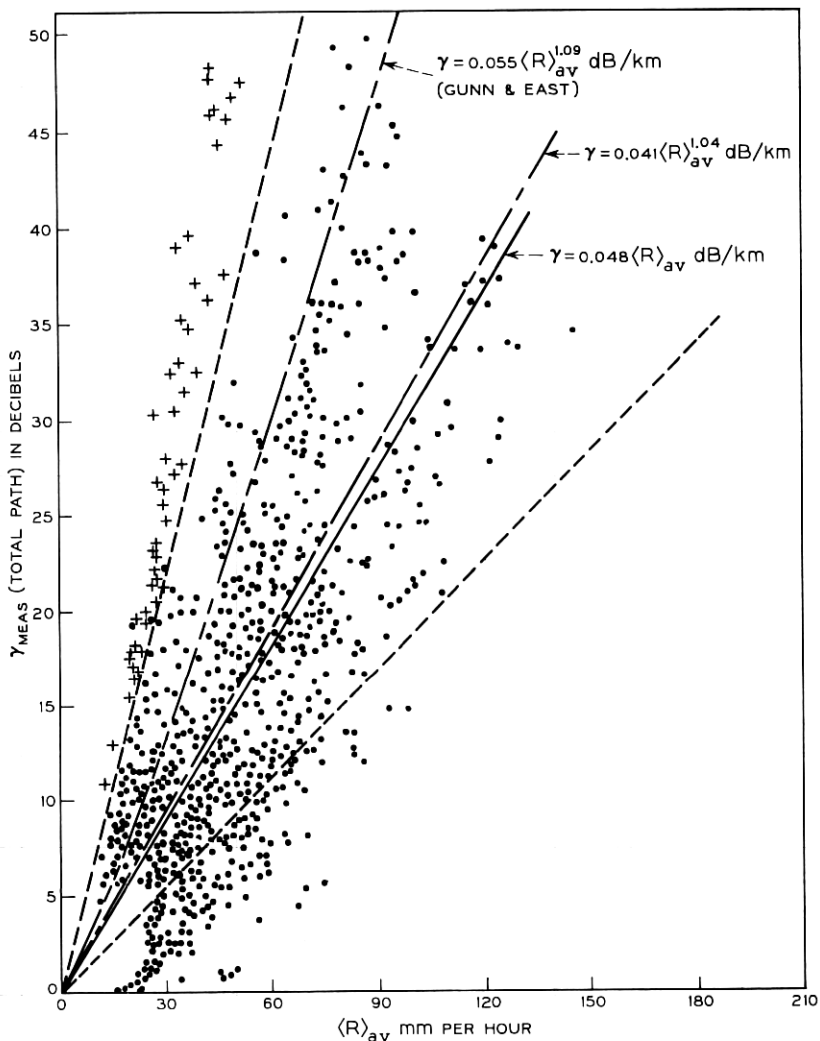
Fig. 7 — Plot of observed attenuation versus average path rain rate, $\langle R \rangle_{av}$, as measured by four gauges with an intergauge spacing of 1.6 km, for all storms during the period June 23 through October 31, 1967. The dashed lines are theoretical maxima and minima. The solid line is a least squares regression. The data points represented by crosses pertain to October 25, 1967.
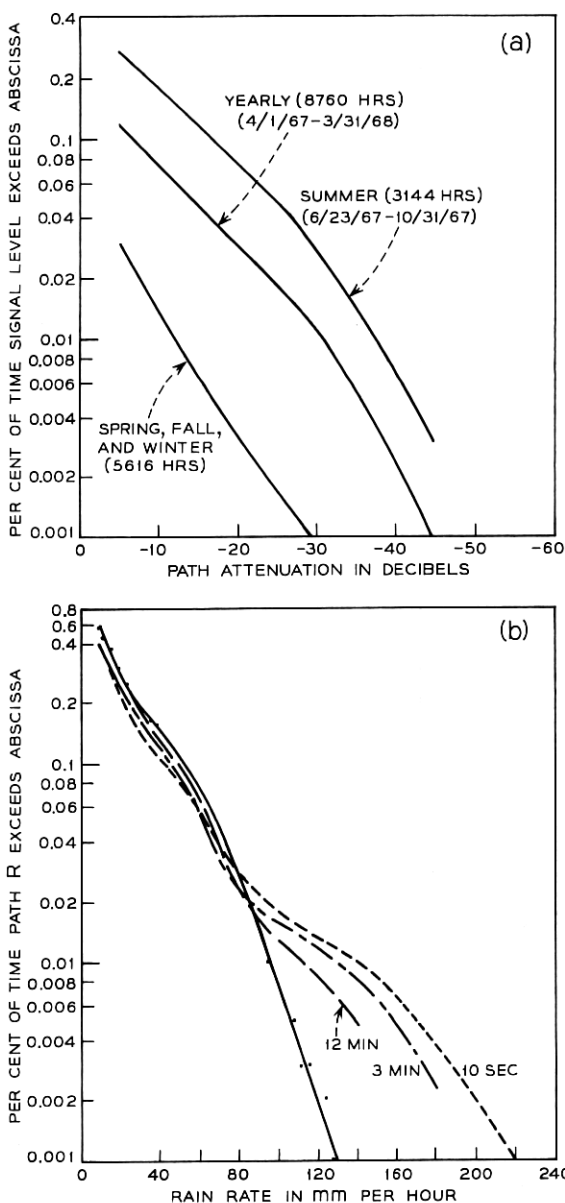
Fig. 8 — (a) Distributions of the percent of time the attenuation exceeds the abscissa for periods of measurements of 3144 hours (summer), 5616 hours winter), and 8760 hours (full year). (b) The percent of time the average rain rate exceeds the abscissa for a total period of 3144 hours (summer).

That the summer distribution is very conservative is readily apparent.

Bussey proposed that there was a relationship between point and space-averaged rainfall rates.[8] If certain, not fully defined restrictions are placed on the length of the path over which the average is taken, system designs based on the point rainfall rates could provide reliable operation. A comparison of point and path averaged distributions is shown in Fig. 8b. The three dashed curves are for point rainfall rate distributions from gauge 25 on the propagation path; averages over time intervals of 10 seconds, 3 minutes, and 12 minutes were used. One sees that, as the time of averaging interval is increased, the tail of the distribution obtained from the point gauge approaches that obtained for the path-average distribution (the solid curve). For rain rates less than about 100 mm per hour, the equivalence between the point and path-average distributions is fairly good; however, for higher rates, the point distribution, even for a 12 minute averaging interval, indicates higher percentage times than the true path-average distribution.

Rather than plotting instantaneous attenuation versus instantaneous path-average rain rate, as has been done in Fig. 7, one can examine the relationship between these two variables by means of the cumulative distributions in Fig. 8. Since the same samples was used in obtaining the distributions of attenuation (Fig. 8a) and average rain rate (Fig. 8b), one can draw a correspondence between the attenuation and the average rain rate for a given probability. For example, at 0.03 per cent probability the average rain rate is 80 mm per hour and the attenuation 30 dB; at the 0.003 per cent value, the average rate is 113 mm per hour and the attenuation 45 dB. For these low probabilities, both distributions are quite linear on the semilogarithmic plot (see Fig. 8). Thus for the 6.4 km path, one obtains

$$\gamma \text{ path} = 0.38 \langle R \rangle_{av} \text{ dB}, \langle R \rangle_{av} > 80 \text{ mm per hour},$$

which results in

$$\gamma = 0.059 \langle R \rangle_{av} \text{ dB/km}, \langle R \rangle_{av} > 80 \text{ mm per hour}.$$

Let us compare this result with the plots of instantaneous data for the 6.4 km path given in Fig. 7. At a path-average rate of 80 mm per hour the Gunn-East curve shows an attenuation of 43 dB; the method of comparison of distributions just discussed, results in an attenuation of 30 dB; and the least squares fit, 26 dB. However the rain gauges are sensors only of points on the path; and since it is more probable

that intense rain cells occur between gauges than on a gauge, the points that fall along the upper end of the Gunn and East curve (the high attenuations) are believed to be associated with actual average rain rates higher than those plotted in the figure. The effect of inadequate sampling of rain rate in the time domain, discussed in the appendix, also leads to conservative estimates of attenuation. Suppose an intense cell produces a rapid peak in the rain rate. If, as a result of sampling error, this peak were not recorded, a given attenuation would be plotted against a rain rate lower than that which actually existed. Again, this means that the high attenuation points are actually associated with average rain rates higher than those plotted in Fig. 7.

The above discussion leads to the question: Based on the present experiment, what is the best relationship between the attenuation and the path-average rain rate? One can only say that at a rate of 100 mm per hour, the attenuation is between five and eight dB per km. However,

$$\gamma = 0.06 \langle R \rangle_{av} \quad \text{dB/km}$$

is considered a working relationship for path-average rates exceeding 50 mm per hour.

Distributions of the duration of fades are plotted in Fig. 9. The ordinate is the percentage of the total number of fades for the 17.8 hours of heavy rain that occured during the period June 23 through October 31. (An example: at the −20 dB level, 5.8 percent of the total number of fades have a duration exceeding five minutes. The total number of fades is 182, therefore 10 fades have durations greater than five minutes at the −20 dB level.

Attenuation by rain at a rate of 100 mm per hour is shown in Fig. 10 for the 8 to 80 GHz band. Most of the plotted points are measurements of the Bell Telephone Laboratories; the measurements at 8 and 15 GHz were made in Canada.[9] All of the points correspond to the heavy average rain rate of 100 mm per hour. In most cases the points were actually measured at that rate; for the others, as indicated by arrows, some extrapolation was made. The solid line is a faired-in fit to the data points.

The broken line is a weighted mean of measured data from many parts of the world assembled by Medhurst for 100 mm per hour rate.[1] The two dashed lines, also shown, represent the maxima and minima of these observations. Clearly, the solid line lies well below the "world" average over all of the band.
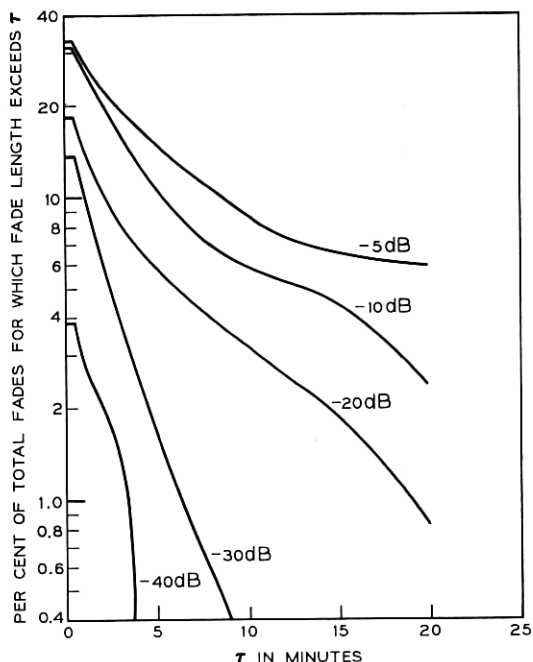
Fig. 9 — Percent of total number of fades for which the fade length exceeds the abscissa. Based on 17.8 hours of rain data and a total of 182 fades.

V. CONCLUSIONS

Calculations using the commonly accepted expression $\gamma = k \sum_i d_i R_i^\alpha$ where $k = 0.055$ dB per kilometer and $\alpha = 1.09$ overestimate the present measurements of 18.5 GHz attenuation by rain. Our data, obtained from four rain gauges with an intergauge spacing of 1.6 km, result in values $k = 0.041$ and $\alpha = 1.04$ over much of the range of observations. The discrepancy may be caused in part by formation of ellipsoidal drops at high rainrates; these would produce lower attenuation for vertical polarization. An incorrect assumption for the fall velocity has a strong influence; as shown by the data for October 25 (Fig. 4) an updraft can produce attenuations above the bounds of conventional predictions. On the other hand, a drop velocity greater than normally assumed in the theory would modify the estimates in a direction toward better agreement with most of the storms we have measured. On the 6.4 km path, the 18.5 GHz attenuation exceeded 30 dB 0.03 percent of the time for this summer season; this path is therefore
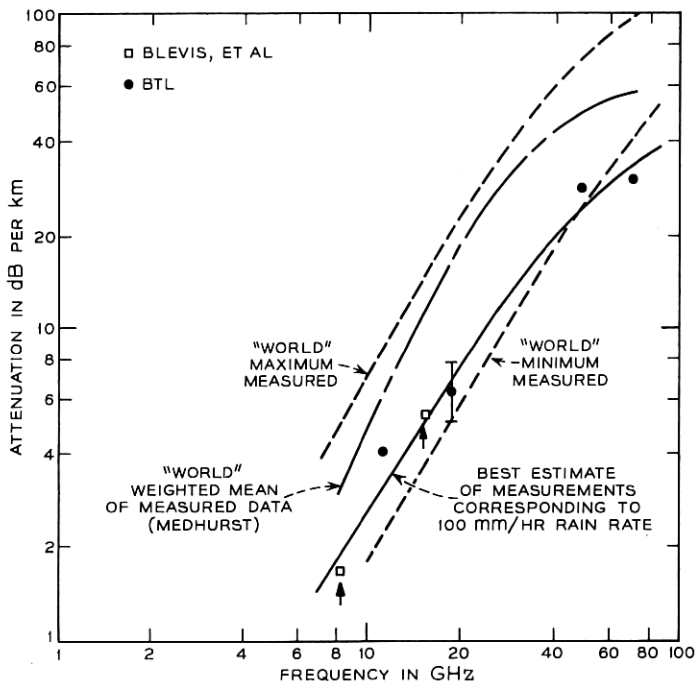
Fig. 10 — The "world" weighted mean from Medhurst is shown as a broken line.[1] The solid line represents data appropriate to an average rainfall rate of 100 mm per hour and is considered the best available basis for prediction in system design. Data plotted:

8 and 15 GHz—Blevis and others[9]
11 GHz—Hathaway and Evans[11]
18.5 GHz—Semplak and Turrin (present data).
48 and 70 GHz—Hogg.[12]

too long for the repeater spacing in a conventional system at this frequency in the New Jersey climate.* For the present sample of data, the average rain rate on the 6.4 km path exceeded 100 mm per hour 0.008 percent of the time; however, point rates in excess of 280 mm per hour have been observed for very short periods. All fades observed to date have been associated with rainfall; thus no "selective fading" has as yet been observed on this 6.4 km path.

VI. ACKNOWLEDGMENTS

The authors are grateful to D. C. Hogg for helpful discussions and to Mrs. E. Kerschbaumer for the computations. The assistance of H. A.

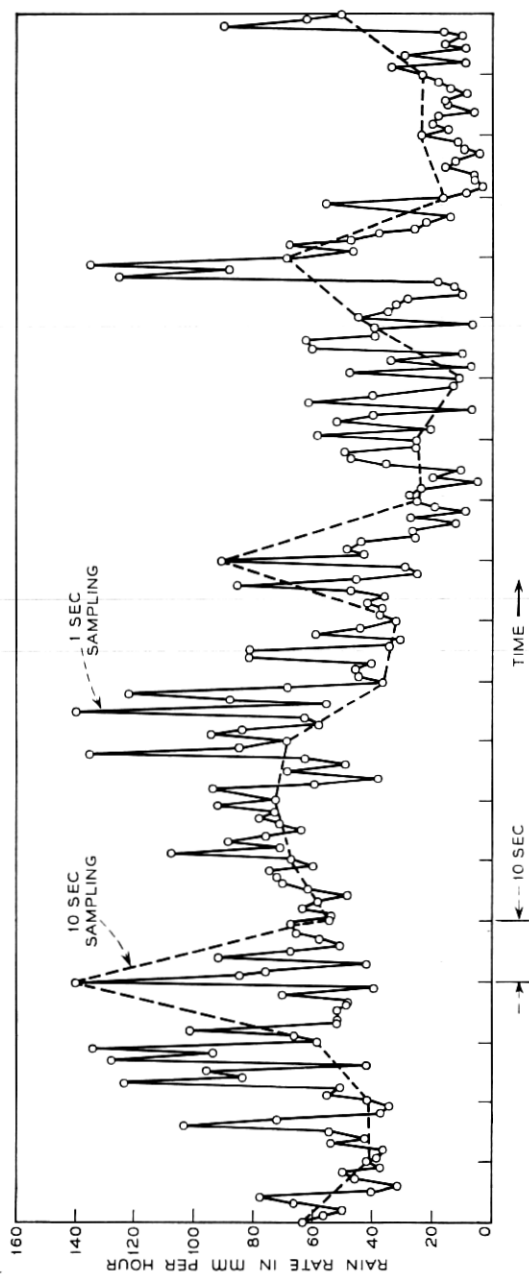* For a discussion of path-diversity systems see Ref. 10.

Fig. 11 — Comparison of one and ten second sampling of rain gauge data.

APPENDIX A

Effect of Temporal Sampling Error in the Raingauge Data

As discussed in a companion paper, the output of the individual rain gauges in the network are sampled and recorded once every ten seconds.[3] In addition, one of the gauges (grid 33 of Fig. 1) is sampled and recorded every second. A portion of the recorded one second sampling data from this gauge for the storm of July 21, 1967 (Fig. 2a) are shown by the solid line of Fig. 11. The dashed line connects the normal 10 second sampling data points from this gauge; it is apparent that 10 second sampling misses many of the peaks shown by the one second sampling. However cumulative distributions of both the one (solid line) and ten second samplings (dashed line) for this storm, whose duration was thirteen minutes, are shown as Fig. 12; one can readily see that the distributions are identical out to rain rates of the order 100 mm per hour. For rates greater than 100 mm per hour, the ten second sampling tends to be conservative. Another cumulative distribution based on a ten second sampling period of this data and
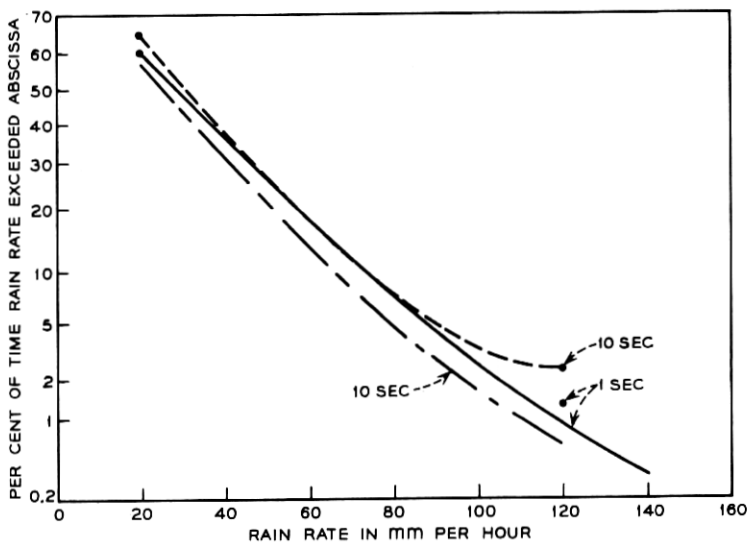

Fig. 12 — Cumulative distributions of rain fall rates based on one and ten second sampling.

selected in a manner such that a minimum of one second peaks would be encountered is shown by the broken line on this figure. Here again this result is not too different from the one second sampling in Fig. 12. Both ten second distributions straddle the one second distribution.

REFERENCES

1. Medhurst, R. G., "Rainfall Attenuation of Centimeter Waves: Comparison of Theory and Experiment," IEEE Trans. Antennas and Propagation, *AP-13*, No. 4 (July 1965), pp. 550–564.
2. Semplak, R. A., "Gauge for Continuously Measuring Rate of Rain Fall," Rev. of Sci. Instruments, *37*, No. 11 (November 1966), pp. 1554–1558.
3. Semplak, R. A., and Keller, H. E., "A Dense Network for Rapid Measurement of Rainfall Rate," B.S.T.J., this issue, pp. 1745–1756.
4. Croney, J., and Worowcow, A., "A True IF Logarithmic Amplifier Using Twin-Gain Stages," REE, *32*, No. 3 (September 1966), pp. 149–155.
5. Gunn, K. L. S., and East, T. W. R., "The Microwave Properties of Precipitation Particles," J. Royal Meteorological Soc., *80*, 1954, pp. 522–545.
6. Oguchi, T., "Attenuation of Electromagnetic Wave Due to Rain with Distorted Rain Drops," J. of the Radio Res. Labs (Tokyo), *7*, No. 33 (September 1960), pp. 467–485.
7. Berry, F. A., Jr., Bollay, E., and Beers, N. R., *Handbook of Meterology*, New York: McGraw-Hill, 1945, pp. 638ff.
8. Bussey, H. E., "Microwave Attenuation Statistics Estimated from Rainfall and Water Vapor Statistics," Proc. IRE, *38*, No. 7 (July 1950), pp. 781–785.
9. Blevis, B. C., Dohoo, R. M., and McCormick, K. S., "Measurements of Rainfall Attenuation at 8 and 15 GHz," IEEE Trans. Antennas and Propagation, *AP-15*, No. 3 (May 1967), pp. 394–403.
10. Hogg, D. C., "Path Diversity in Propagation of Millimeter Waves through Rain," IEEE Trans. *T-AP 15*, No. 3 (May 1967), pp. 410–415.
11. Hathaway, S. D., and Evans, H. W., "Radio Attenuation at 11 Kmc and Implications Affecting Relay System Engineering," B.S.T.J., *38*, No. 1 (January 1959), pp. 73–98.
12. Hogg, D. C., "Millimeter-Wave Communication through the Atmosphere," Science, *159*, No. 3810 (January 1968), pp. 39–46.